

## Single crystal diamond detector measurements of deuterium-deuterium and deuterium-tritium neutrons in Joint European Torus fusion plasmas

C. Cazzaniga, E. Andersson Sundén, F. Binda, G. Croci, G. Ericsson, L. Giacomelli, G. Gorini, E. Griesmayer, G. Grosso, G. Kaveney, M. Nocente, E. Perelli Cippo, M. Rebai, B. Syme, M. Tardocchi, and JET-EFDA Contributors

Citation: [Review of Scientific Instruments](#) **85**, 043506 (2014); doi: 10.1063/1.4870584

View online: <https://doi.org/10.1063/1.4870584>

View Table of Contents: <http://aip.scitation.org/toc/rsi/85/4>

Published by the [American Institute of Physics](#)

---

### Articles you may be interested in

[A diamond based neutron spectrometer for diagnostics of deuterium-tritium fusion plasmas](#)

[Review of Scientific Instruments](#) **85**, 11E101 (2014); 10.1063/1.4885356

[Neutron emission spectroscopy of DT plasmas at enhanced energy resolution with diamond detectors](#)

[Review of Scientific Instruments](#) **87**, 11D822 (2016); 10.1063/1.4960307

[Response function of single crystal synthetic diamond detectors to 1-4 MeV neutrons for spectroscopy of D plasmas](#)

[Review of Scientific Instruments](#) **87**, 11D823 (2016); 10.1063/1.4960490

[First neutron spectroscopy measurements with a pixelated diamond detector at JET](#)

[Review of Scientific Instruments](#) **87**, 11D833 (2016); 10.1063/1.4961557

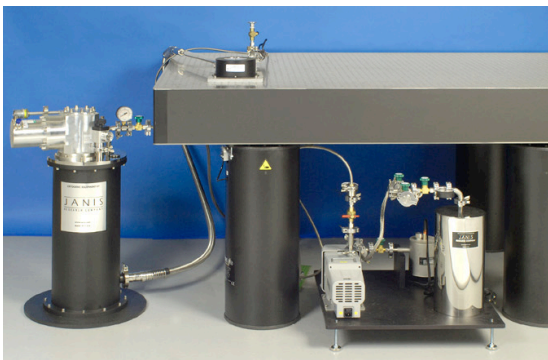
[Fast ion energy distribution from third harmonic radio frequency heating measured with a single crystal diamond detector at the Joint European Torus](#)

[Review of Scientific Instruments](#) **86**, 103501 (2015); 10.1063/1.4931755

[Energy resolution of gamma-ray spectroscopy of JET plasmas with a LaBr<sub>3</sub> scintillator detector and digital data acquisition](#)

[Review of Scientific Instruments](#) **81**, 10D321 (2010); 10.1063/1.3501386

---



# JANIS

**Rising LHe costs? Janis has a solution.**  
Janis' Recirculating Cryocooler eliminates the use of Liquid Helium for "wet" cryogenic systems.

[sales@janis.com](mailto:sales@janis.com) [www.janis.com](http://www.janis.com) **Click for more information.**

# Single crystal diamond detector measurements of deuterium-deuterium and deuterium-tritium neutrons in Joint European Torus fusion plasmas

C. Cazzaniga,<sup>1,2,a)</sup> E. Andersson Sundén,<sup>3</sup> F. Binda,<sup>3</sup> G. Croci,<sup>2</sup> G. Ericsson,<sup>3</sup> L. Giacomelli,<sup>1</sup> G. Gorini,<sup>1,2</sup> E. Griesmayer,<sup>4</sup> G. Grosso,<sup>2</sup> G. Kaveney,<sup>5</sup> M. Nocente,<sup>1,2</sup> E. Perelli Cippo,<sup>2</sup> M. Rebai,<sup>1</sup> B. Syme,<sup>5</sup> M. Tardocchi,<sup>2</sup> and JET-EFDA Contributors<sup>b)</sup>

JET-EFDA, Culham Science Centre, Abingdon OX14 3DB, United Kingdom

<sup>1</sup>Department of Physics "G. Occhialini," University of Milano Bicocca, Piazza della Scienza 3, Milano, Italy

<sup>2</sup>Istituto di Fisica del Plasma, Associazione EURATOM-ENEA-CNR, via Roberto Cozzi 53, Milano, Italy

<sup>3</sup>Department of Physics and Astronomy, EURATOM-VR Association, Uppsala University, Uppsala, Sweden

<sup>4</sup>Atominstytut, Vienna University of Technology, Austria

<sup>5</sup>Culham Centre for Fusion Energy, Culham OX143DB, United Kingdom

(Received 31 January 2014; accepted 23 March 2014; published online 11 April 2014)

First simultaneous measurements of deuterium-deuterium (DD) and deuterium-tritium neutrons from deuterium plasmas using a Single crystal Diamond Detector are presented in this paper. The measurements were performed at JET with a dedicated electronic chain that combined high count rate capabilities and high energy resolution. The deposited energy spectrum from DD neutrons was successfully reproduced by means of Monte Carlo calculations of the detector response function and simulations of neutron emission from the plasma, including background contributions. The reported results are of relevance for the development of compact neutron detectors with spectroscopy capabilities for installation in camera systems of present and future high power fusion experiments. [<http://dx.doi.org/10.1063/1.4870584>]

## I. INTRODUCTION

Single crystal Diamond Detectors (SDDs) are artificially produced by chemical vapor deposition.<sup>1</sup> In recent years they have been successfully used for fast neutron measurements in the MeV range mostly at spallation sources,<sup>2–5</sup> where spectral measurements were demonstrated in time of flight experiments. SDDs are interesting candidates also for measurements of the 2.5 MeV and 14 MeV neutron energy spectrum from fusion plasmas of tokamak experiments, particularly in next step devices, such as ITER. Here, advantage can be taken of the high neutron fluxes ( $10^9$  n cm<sup>-2</sup> s<sup>-1</sup>), which enable measurements at high counting rates (MHz) and, thus, temporal resolution (a few ms). Besides, the compact dimensions and radiation resistance of SDDs make them particularly interesting as detectors for camera systems with spectroscopy capabilities, thanks to their high energy resolution ( $\approx 2\%$  at 5 MeV).

As far as neutron spectroscopy applications of SDDs are concerned, a distinction must be made between neutrons of energy below and above 6 MeV, due to the different response function of the instrument in these energy ranges. Above 6 MeV, neutron spectroscopy is enabled by the  $^{12}\text{C}(n,\alpha)^9\text{Be}$  reaction (energy threshold: 6.17 MeV) between the incoming neutrons and carbon nuclei of the diamond crystal. The  $\alpha$  particle energy is deposited in the device and results in a peak, whose mean position and shape depend on the incoming neutron energies. For example, 14 MeV neutrons from

deuterium-tritium (DT) plasmas would be manifested as a peak at mean energy  $E_0 = 8.5$  MeV with width proportional to the square root of the plasma temperature  $T$ .<sup>6</sup> Measurements of 14 MeV neutrons were performed in tokamak experiments with DT plasmas using natural diamond detectors and are reported in Refs. 7–9.

For neutron energies below 6 MeV, instead, the  $^{12}\text{C}(n,\alpha)^9\text{Be}$  reaction is forbidden by kinematics and the main reaction channel is neutron elastic scattering on  $^{12}\text{C}$  nuclei. The  $^{12}\text{C}$  recoil nuclei are stopped in the detector and, for a monochromatic neutron beam, their spectrum appears as a continuous distribution ending at the maximum recoil energy transferred to  $^{12}\text{C}$ , which is proportional to the incoming neutron energy. Measurements of the SDD response in this energy range, as well as for  $E_n > 6$  MeV, were performed at accelerator facilities and are reported in the literature.<sup>10–12</sup> The simultaneous detection of 2.5 and 14 MeV neutrons from a fusion plasma using a lithium coated SDD is reported in Ref. 13. In this experiment, the detection efficiency of the device was boosted by the  $^6\text{Li}(n,\alpha)\text{T}$  reaction in the coating which, however, resulted in a loss of spectroscopy information on 2.5 MeV neutrons.

In this work we present the first simultaneous spectroscopy measurements of 2.5 and 14 MeV neutrons from a deuterium-deuterium (DD) fusion plasma in a tokamak environment using a bare SDD. The measurements were performed at JET with a fast acquisition chain optimized for high rate applications and are interpreted in terms of components of the neutron emission spectrum together with the simulated SDD response function. Advantages of SDDs over other techniques based on compact detectors for neutron measurements in tokamak experiments are finally illustrated.

<sup>a)</sup>carlo.cazzaniga@mib.infn.it

<sup>b)</sup>See the Appendix of F. Romanelli *et al.*, Proceedings of the 24th IAEA Fusion Energy Conference 2012, San Diego, USA.

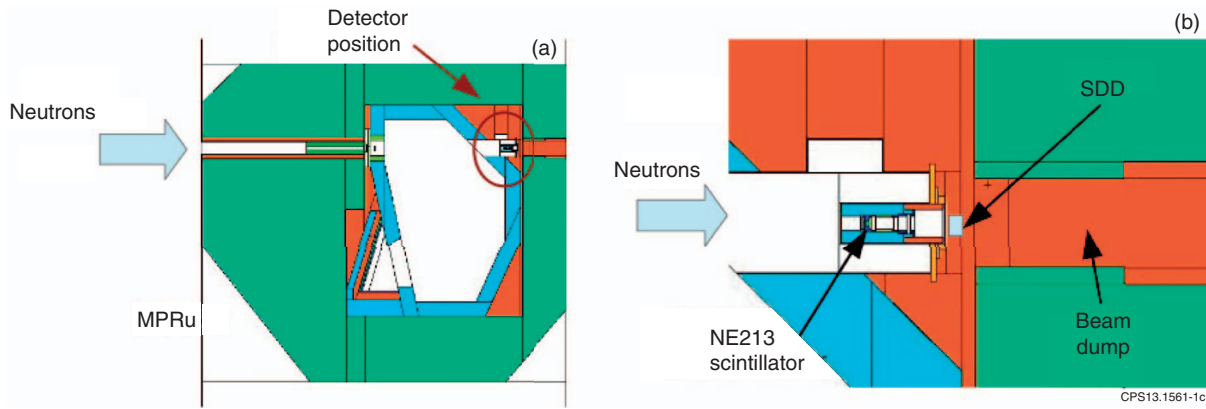


FIG. 1. (a) Schematics of the SDD detector arrangement inside the radiation shielding of MPRu spectrometer. The direction of the neutrons produced by the plasma is indicated by the arrow. (b) Zoom of the detector position in front of the MPRu beam dump.

## II. EXPERIMENTAL SETUP

An artificially grown SDD was installed in the JET Torus Hall on a collimated Line of Sight (LoS) shared with other neutron diagnostics, the MPRu proton-recoil neutron spectrometer and the NE213 scintillator.<sup>14–17</sup> Fig. 1 shows the position of the detector inside the MPRu radiation shielding as in the MCNP model<sup>18</sup> used for the calculations presented in Sec. IV. The installed diamond detector had a nominal active volume of the  $4.7 \times 4.7 \text{ mm}^2$  (surface area)  $\times 0.5 \text{ mm}$  (thickness) with 4.5 mm diameter aluminium electrical contacts.

Two separate read-out electronic chains (see Fig. 2) were developed to measure, at the same time, DD (2.5 MeV) and DT (14 MeV) neutrons. This was needed since the energy deposition for DD neutrons, due to carbon recoil, is about 20 times less than the energy deposition of DT neutrons via the  $(n, \alpha)$  reaction. Both chains shared a fast charge preamplifier CIVIDEC c6<sup>22</sup> as a first amplification stage. The latter was placed about 20 cm away from the diamond detector, without intercepting the neutron beam. A 120 meter BNC cable was laid down from the preamplifier to the JET Diagnostic Hall, where signals from the diamond detector were recorded. The signal FWHM from an  $\alpha$ -particle of the calibration source, measured after the long BNC cable, was 20 ns (see Fig. 3(a)). For 2.5 MeV neutron measurements a second amplification stage, consisting of a 20 dB current amplifier CIVIDEC c1,<sup>22</sup> was installed right after the first preamplifier in the Torus Hall. Fig. 3(b) shows the signal from 2.5 MeV neutrons after the second amplification stage. Clearly, there is a worse signal-to-noise ratio compared to the pulse from the calibration source of Fig. 3(a), but the FWHM of the sig-

nal is still about 20 ns, which shows that the current amplifier did not introduce any significant shaping that could alter the fast temporal properties of the signal. Preserving fast signals is essential in view of high rate measurements in the JET DT campaign.

A four channel, 1 GHz, 10 bit CAEN waveform digitizer model DT5751 (input range: 0–1 V) was used to record the signals from both electronic chains in the Diagnostic Hall.<sup>23</sup> The acquisition was triggered by the JET “pre”-signal, that is produced 40 s before each plasma discharge. The Pulse Height Spectrum (PHS) corresponding to each discharge was reconstructed off-line with a software based on a trapezoidal filter algorithm.<sup>24</sup>

A calibration triple- $\alpha$  source ( $^{241}\text{Am}$ ,  $^{239}\text{Pu}$ , and  $^{244}\text{Cm}$ ) was placed in front of the detector, providing a counting rate  $< 10 \text{ Hz}$ . A typical calibration spectrum, collected in 60 min without neutron emission from the plasma, is shown in Fig. 4. It has to be considered in the calibration a calculated energy loss in air of 0.39 MeV. An energy resolution (FWHM/E) of 2.2% can be measured at 5.2 MeV. This value is acceptable for fusion spectroscopy applications, as it is smaller than the kinematic broadening of the thermal emission peak from DT plasmas (between 2% and 10% for plasma temperatures in the range 3–10 keV<sup>6</sup>). For 2.5 MeV neutron measurements, which correspond to a maximum of 0.8 MeV of deposited Energy, the energy resolution of the SDD is assumed to be 8%. This value was extrapolated from the resolution determined experimentally using a  $^{137}\text{Cs}$   $\gamma$ -ray source.

## III. NEUTRON MEASUREMENTS ON JET DEUTERIUM PLASMAS

Neutron measurements (2.5 MeV) have been performed in deuterium plasmas from July 2013 during the JET C31 campaign. A clear evidence that the signals measured by the SDD detector were due to fusion neutrons was obtained by comparing the counts measured by the SDD with the neutron yield observed by the standard JET neutron diagnostics. The result is shown in Fig. 5, where each data point represents an individual discharge performed on 13 August 2013. The SDD measurements had a low energy threshold

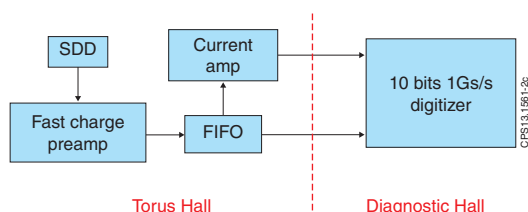


FIG. 2. Schematics of the read-out electronics used for SDD measurements at JET.

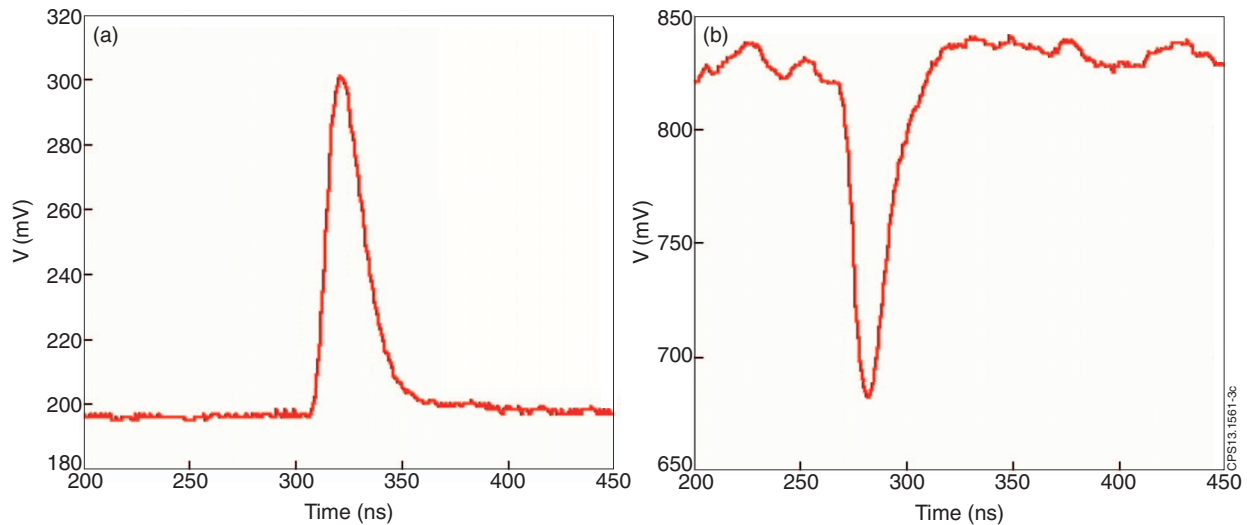


FIG. 3. Signals from an  $\alpha$  particle of the calibration source after the BNC cable in the Diagnostic Hall (a) and from a 2.5 MeV neutron after the second amplification stage (see text for details) (b).

corresponding to a deposited energy  $E_d = 0.3$  MeV and are shown in the figure versus the total neutron yield measured by the JET fission chamber diagnostics.<sup>25</sup> There is clear linear correlation between the two set of data (correlation coefficient  $R^2 = 0.9988$ ) with a proportionality constant of  $4.5 \times 10^{-13}$ . This small value results from the combined contribution of neutron transport from the plasma to the detector position and of the detector efficiency, which can be calculated to be about 1.4% for 2.45 MeV neutrons, based on the  $n+^{12}\text{C}$  nuclear elastic scattering cross sections.<sup>26</sup> A comparison between the counts recorded by SDD and a NE213 liquid scintillator (active volume  $1 \text{ cm}^2 \times 1 \text{ cm}$ ) placed in front of the SDD along the same LOS (see Figure 1) is presented in Fig. 5(b) for the same set of discharges of Fig. 5(a). Again, we find a very good correlation between the two set of data ( $R^2 = 0.9986$ ). The NE213/SDD efficiency ratio, derived from a linear fit to the data, is about 50/1.

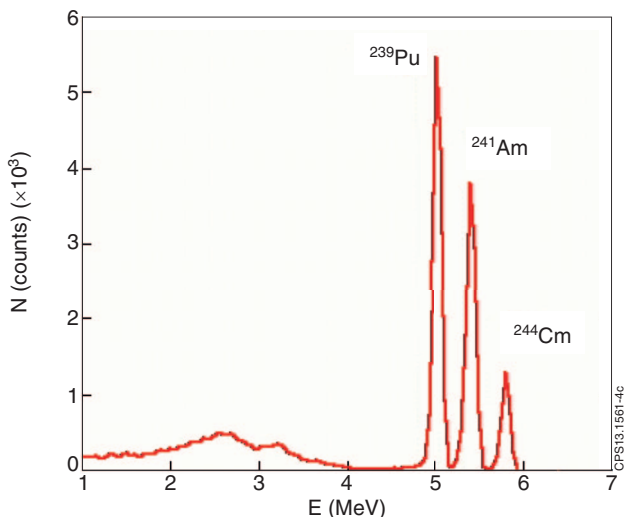


FIG. 4. Energy spectrum of a calibration triple- $\alpha$  source measured with the SDD in the final setup at JET.

The neutron emission time trace measured by SDD is compared with that from the JET fission chambers for a specific JET discharge (#84476) in Fig. 6. The latter is a discharge with average Neutral Beam Injection (NBI) power of about 15 MW. Data for SDD are shown every 0.5 s to mitigate the statistical fluctuations arising from the low (a few hundred Hz) counting rates observed in deuterium plasmas at the detector location. The good agreement between the two set of data confirms the validity of the SDD measurements.

We now move to the analysis of the measured PHS from DD neutrons. This is shown for a single JET discharge (#84476) in Fig 7(a) and for 45 similar discharges in Fig. 7(b) as a function of the charged particle energy released in the detector  $E_d$ . All these experiments were deuterium plasmas with NBI power from 12 MW to 20 MW. Qualitatively, the PHS has the characteristic box shape expected from the energy distribution of the  $^{12}\text{C}$  recoil ions. The shoulder of the PHS is at 0.69 MeV, which correctly corresponds to the maximum energy deposited by back-scattering of 2.5 MeV neutrons on Carbon.<sup>27</sup> The broadening of the edge is due to the combined contribution of the finite detector energy resolution and of Doppler broadening from plasma kinematics (see Sec. IV).

It can be noted here that a deuterium plasma offers the opportunity to also perform measurements of 14 MeV neutrons. These come from the burn up of tritons on deuterium. Tritons are in turn produced by the  $d + d \rightarrow p + t$  reaction, which has about the same cross section as  $d + d \rightarrow n + ^3\text{He}$ . At JET, the 14 MeV, Triton Burn up Neutron emission (TBN) in deuterium plasmas is estimated to be about 1% of that at 2.5 MeV.<sup>28–30</sup> In order to observe TBN emission we have summed all discharges performed at JET during more than 1 month of operations with the result shown in Fig. 8. The 14 MeV TBN emission is manifested by the appearance of the  $(n,\alpha)$  peak which, as stated in the introduction, is the dominant neutron interaction channel for  $E_n > 6.2$  MeV. The significant width of the peak (about 2 MeV FWHM) reflects the triton slowing down distribution and is in good agreement

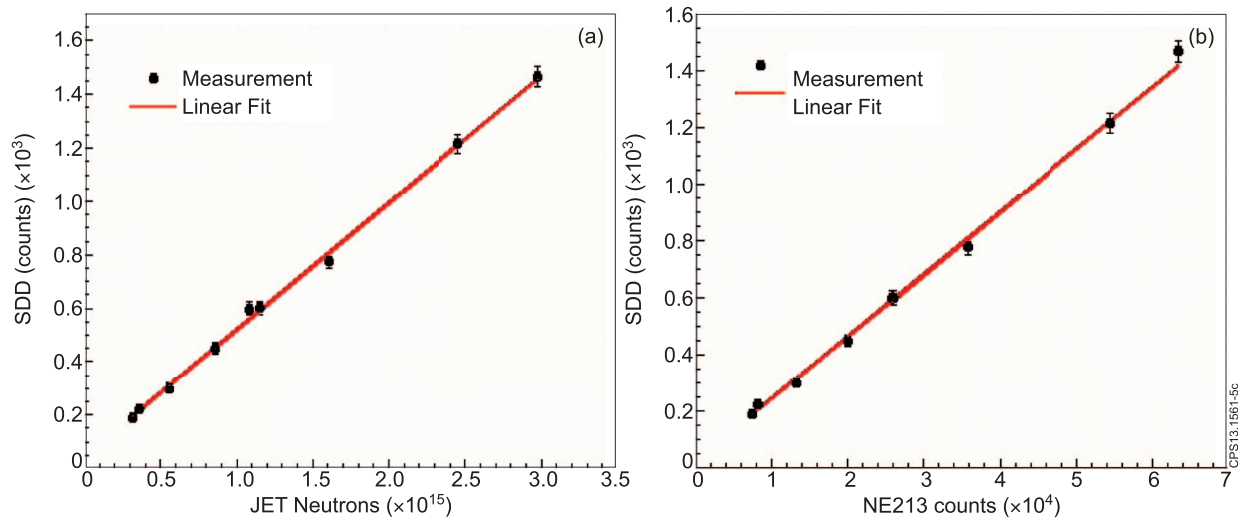


FIG. 5. (a) Neutron counts measured by SDD versus the JET total neutron yield as derived from fission chambers. Each point corresponds to an individual discharge. (b) Neutron counts measured by SDD and by a NE213 liquid scintillator along the same line of sight.

with calculations for JET (see Figure 7 of Ref. 29). The fit is obtained by comparison of a Gaussian function in terms of Cash statistics.<sup>31</sup> It can be noted that a shoulder appears for  $E_d < 8$  MeV; this continuous is due to the  $^{12}\text{C}(n,n)3\alpha$  reaction, as it is discussed in more details in Ref. 11.

#### IV. QUANTITATIVE ANALYSIS OF THE DEPOSITED ENERGY SPECTRUM

The measured PHS can be analyzed to separate different neutron emission components from the plasma. To this end, one must first determine the background due to the calibration source. This was measured, without plasma emission, for about 130 min with the results shown in Fig. 9.

A MCNP model<sup>18</sup> was developed to simulate the detector response function to mono-energetic neutrons up to 4 MeV with an energy step of 100 keV. The model geometry consisted of the bare diamond volume and aluminum contacts.

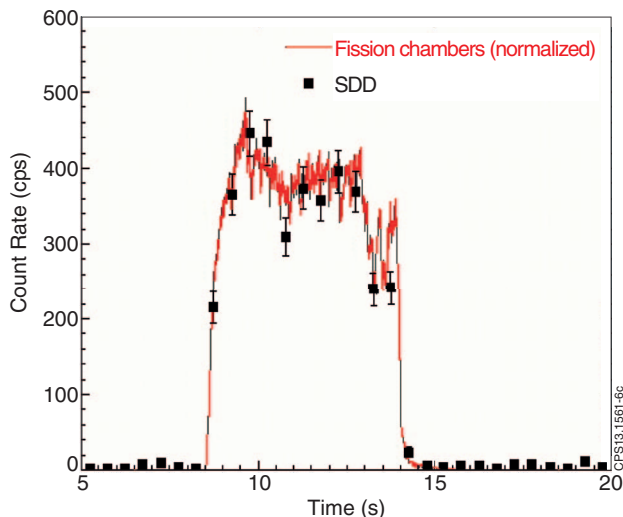


FIG. 6. Time trace of neutron emission measured by SDD and by the JET fission chambers for discharge #84476.

Mono-energetic neutrons at different energies were generated and impinged on the front part of the detector. The same geometry was used to simulate the response to background  $\gamma$ -rays (see below). The resulting response function was convoluted with simulations of increasing complexity of the neutron emission spectrum from the plasma for comparison with measurements, as shown in Fig. 10. As a first step, we assumed the neutron spectrum to uniquely consist of mono-energetic neutrons at  $E = 2.45$  MeV (green dashed curve). This however provided an unsatisfactory description of the measured PHS, both in the flat region corresponding to low recoil energies and for the high energy shoulder.

As a second step, we used a more detailed model for neutron emission from NBI heated plasmas. In this model, neutron emission is described in terms of three components: the thermal, that arises from reaction within the thermal (Maxwellian) plasma population; the beam-plasma, which originates from beam ions reacting with thermal ions; and the beam-beam, that is due to fusion reactions among deuterons of the beam. All of these components were calculated with the Monte Carlo code GENESIS, which can determine the neutron and  $\gamma$ -ray emission spectrum from the plasma using as input the reactant distribution functions.<sup>32–35</sup> A half-box model was adopted to represent the beam population.<sup>36</sup> The output from GENESIS was in turn validated by comparison with measurements from the TOFOR neutron spectrometer for a few discharges.<sup>19–21</sup>

As the summed spectrum of Figure 10 included plasmas with different NBI injection energies (ranging from 80 keV to 120 keV), separate simulations were correspondingly performed and then combined with weights proportional to the actual NBI power mix used in the experiments. The finite energy resolution of the SDD was taken into account by convolution with a Gaussian of  $\text{FWHM} = 8\%$ . This value was extrapolated from the resolution determined experimentally using a  $^{137}\text{Cs}$   $\gamma$ -ray source. The result of the fit is shown by the red curve in Fig. 10. The high energy shoulder is now well described, but there is a significant excess of data in the low

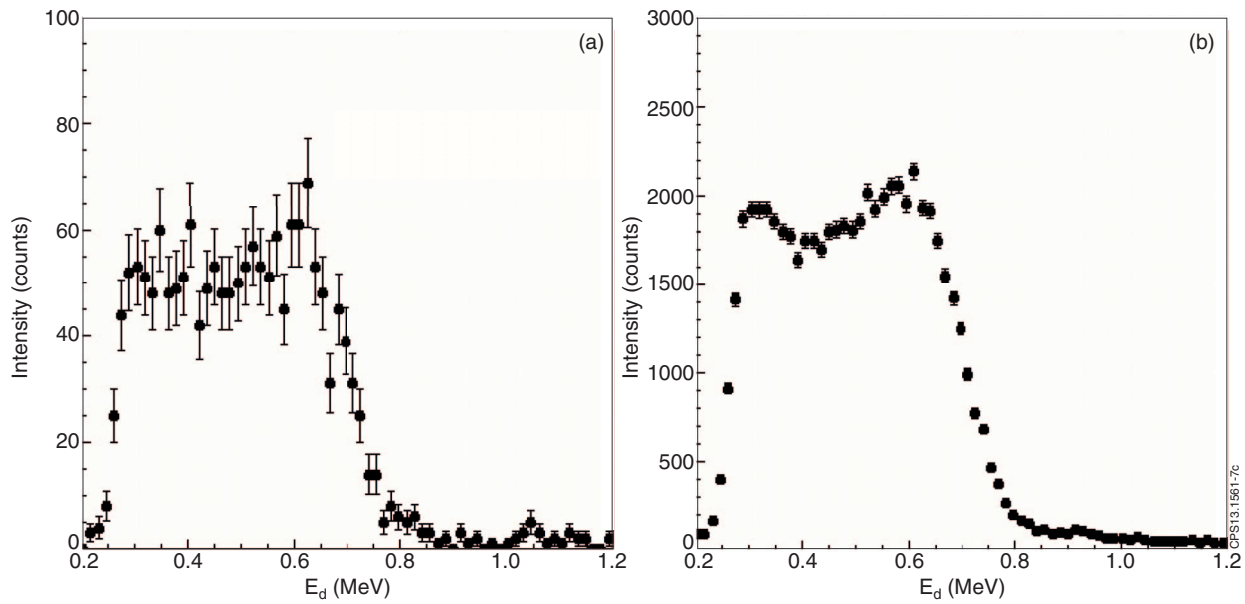


FIG. 7. (a) Pulse height spectrum from DD fusion neutrons measured by SDD in discharge #84476 at JET, as a function of the charged particle energy released in the detector  $E_d$ . (b) Pulse height spectrum from the sum of 45 similar JET discharges.

energy part of the spectrum that is not accounted for by the simulation.

This discrepancy can be solved by considering the background contributions from  $\gamma$ -rays and scattered neutrons to the measured spectrum. To this end, the MCNP model for MPRu (Fig. 1) was used to calculate  $\gamma$ -ray production in the beam dump and the scattering of the incoming neutrons along the MPRu line of sight. The contributions of these two background sources are shown in Figure 11 in linear and log scale. Neutron scattering results in an excess of low energy neutrons that show up as a component of significant intensity up to  $E_d = 0.5$  MeV, with a rapid fall off at higher energies. Gamma-ray induced events in the SDD have a clear exponential shape.

The complete description of the measured data (solid line of Fig. 11) thus included four contributions: (1) a primary component due to d+d neutrons emitted from the plasma and

that reach the detector, as in Fig. 10; (2) scattered neutrons and (3)  $\gamma$ -rays produced by the interaction of the primary neutrons with the MPRu LoS; (4) background events from the triple- $\alpha$  calibration source, normalized to measurement time. Two normalization parameters only were determined by the fit, namely the absolute intensity of the primary neutron component and the amount of scattered neutrons. The scattered neutron/background  $\gamma$ -ray ratio was constrained to the value found by MCNP and confirmed by the NE213 measurements, which can distinguish signals from neutrons and  $\gamma$ -rays from their different pulse shapes. This allows for minimizing the number of free parameters in the fit. The background intensity from the triple- $\alpha$  source was known independently

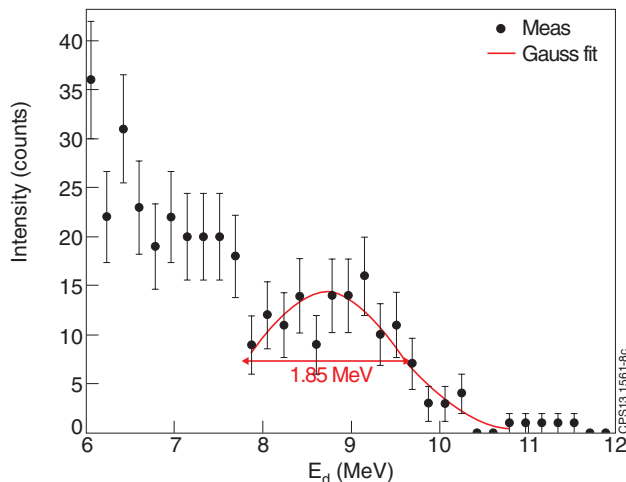


FIG. 8. Measured pulse height spectrum from triton burn up neutrons in deuterium plasmas at JET. Data from all discharges during 1 month of operations at JET were summed. The FWHM of the  $(n, \alpha)$  peak is indicated in the figure.

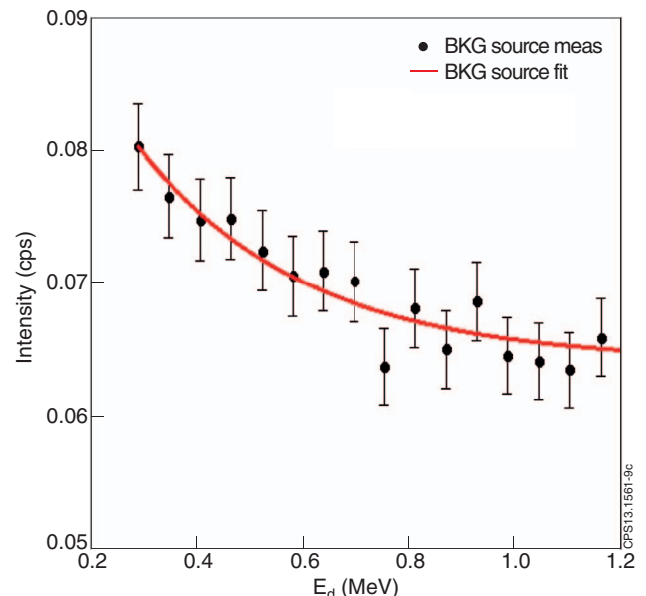


FIG. 9. Background energy spectrum due to the calibration source normalized to the measurement time.

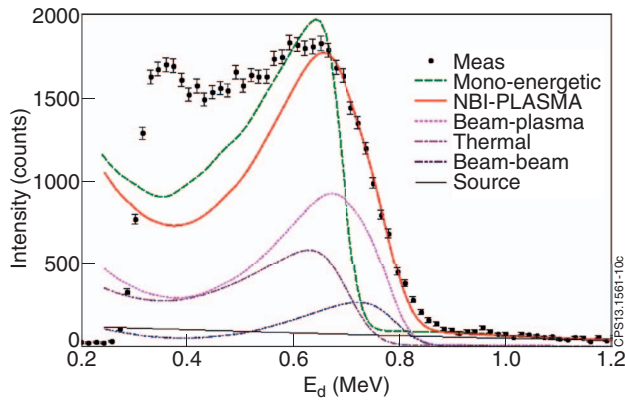


FIG. 10. Measured SDD pulse height spectrum compared to simulations of the expected signal from different neutron emission models. The green dashed curve corresponds to mono-energetic neutrons at  $E = 2.45$  MeV. The solid red curve is instead the result of a neutron emission model for NBI injection, which includes thermal (pink dotted), beam-plasma (violet dotted), and beam-beam (blue dotted) reactions (see text for details). The background counting level from the triple- $\alpha$  calibration source is normalized to the measurement time.

from a separate measurement and re-scaled to the actual measurement time during the plasma discharges. With all four components included, we find a good agreement between measurements and data. In particular, neutron scatter-

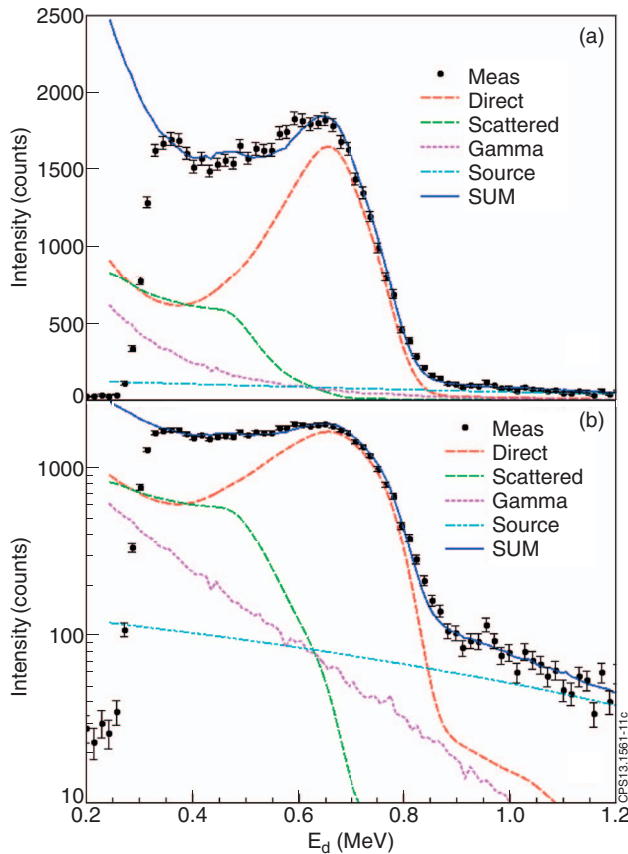


FIG. 11. Measured PHS spectrum from a set of NBI plasmas as compared to simulations in linear (a) and logarithmic (b) scale. The simulated spectrum is the sum of four components: (1) a primary component due to  $d + d$  neutrons emitted from the plasma and that reach the detector; (2) scattered neutrons and (3)  $\gamma$ -rays produced by the interaction of the primary neutrons with the MPRu LoS; and (4) background events from the calibration source, normalized to measurement time.

ing amounts to 35% of the total, with background  $\gamma$ -rays contributing to about 20%. The contribution of the background components is mostly at low energies (say,  $E_d < 0.5$  MeV) negligible in the shoulder of the PHS, whose shape is completely determined by direct (primary)  $d+d$  neutrons.

## V. DISCUSSION AND OUTLOOK

Artificial diamonds can play a role as compact neutron detectors with spectroscopy capabilities for fusion applications, together with other devices such as NE213 scintillators.<sup>37–39</sup> Compact detectors are of importance for use in camera systems of a burning plasma experiment, where there is limited space for implementation of more complex devices such as dedicated spectrometers for 2.5 and 14 MeV neutrons.<sup>14,19</sup> A few points may be raised here to point out advantages and disadvantages of diamond detectors, also in comparison with NE213 scintillator and with reference to DD and DT experiments:

- (i) Both SDD and NE213 feature compact dimensions and high rate capability. The difference in efficiency, which is set by the material volumes commercially available, makes them complementary depending on expected neutron fluxes. The efficiency of SDD can be increased by using a matrix of detectors.
- (ii) The SDD does not suffer significant gain drifts at high counting rates<sup>12,40</sup> and strong magnetic fields. These could instead be of major concerns for a scintillator.
- (iii) NE213 allows for  $n-\gamma$  pulse shape discrimination<sup>41,42</sup> which is not possible with a SDD, that, nevertheless, is fairly insensitive to  $\gamma$ -rays, as demonstrated by these measurements. Besides,  $\gamma$ -ray events mostly concentrate in the low energy part of the spectrum and can thus be discriminated by setting a proper low energy threshold in the PHS.
- (iv) In deuterium plasmas, SDD allows for a good discrimination of direct (primary) and scattered neutrons. For example, setting an energy threshold at  $E_d = 0.5$  MeV (see Fig. 11), would reduce the scattered neutron contribution to only 10% of the direct one. Such improvement in the scattered to direct neutron ratio would enhance the imaging capability of a neutron camera system, and ease the interpretation and analysis of neutron calibrations in a tokamak.
- (v) In DT plasmas, SDD could allow obtaining spectroscopy information from the peak shape of the  $(n,\alpha)$  reaction, providing detailed information on the fuel ion energy distributions. This information could be used for fast ion studies, as demonstrated so far in present tokamaks with dedicated high resolution spectrometers such as MPRu and TOFOR.<sup>43–46</sup> Adding spectroscopy information to a neutron camera system by means of compact detectors would allow for spatially resolved measurements of the fast ion energy distribution in a high performance device.

## VI. CONCLUSIONS

First measurements of the neutron spectrum from deuterium plasmas using a single crystal diamond detector were

presented in this paper. The data were taken at JET by equipping the detector with a fast electronic chain designed to combine high count rate capabilities (up to the MHz range) and good energy resolution ( $\approx 2\%$  at 5 MeV). The observed neutron count rate was successfully correlated to data from other standard neutron rate diagnostics at JET. The deposited energy spectra were measured for both DD and burn-up DT neutrons. Monte Carlo simulations were used to determine the device response function and to interpret the measured pulse height spectrum in terms of components of neutron emission from NBI plasmas, including background contributions. A good agreement was found between calculations and measurements. The results presented here will be the basis for further developments of diamond detectors for neutron diagnostics of JET DD and DT plasmas and in view of burning plasma experiments of the next generation.

## ACKNOWLEDGMENTS

This work was supported by EURATOM and carried out within the framework of the European Fusion Development Agreement. The views and opinions expressed herein do not necessarily reflect those of the European Commission.

- <sup>1</sup>C. Tuve, M. Angelone, V. Bellini, A. Balducci, M. G. Donato, G. Faggio, M. Marinelli *et al.*, "Single crystal diamond detectors grown by chemical vapor deposition," *Nucl. Instrum. Methods Phys. Res., Sect. A* **570**(2), 299–302 (2007).
- <sup>2</sup>A. Pietropaolo, C. Andreani, M. Rebai, L. Giacomelli, G. Gorini, E. Perelli Cippo, M. Tardocchi *et al.*, "Single-crystal diamond detector for time-resolved measurements of a pulsed fast-neutron beam," *EPL* **92**(6), 68003 (2010).
- <sup>3</sup>A. Pietropaolo, C. Andreani, M. Rebai, L. Giacomelli, G. Gorini, E. Perelli Cippo, M. Tardocchi *et al.*, "Fission diamond detectors for fast-neutron ToF spectroscopy," *EPL* **94**(6), 62001 (2011).
- <sup>4</sup>M. Rebai, C. Andreani, A. Fazzi, C. D. Frost, L. Giacomelli, G. Gorini, E. Milani *et al.*, "Fission diamond detector tests at the ISIS spallation neutron source," *Nucl. Phys. B, Proc. Suppl.* **215**(1), 313–315 (2011).
- <sup>5</sup>M. Rebai, L. Giacomelli, C. Andreani, A. Fazzi, C. D. Frost, E. Perelli Cippo, A. Pietropaolo *et al.*, "Diamond detectors for fast neutron measurements at pulsed spallation sources," *J. Instrum.* **7**(05), C05015 (2012).
- <sup>6</sup>Günther Lehner and Pohl Frank, "Reaktionsneutronen als hilfsmittel der plasmadiagnostik," *Z. Phys.* **207**(1), 83–104 (1967).
- <sup>7</sup>A. V. Krasilnikov, E. A. Azizov, A. L. Roquemore, V. S. Khrunov, and K. M. Young, "TFTR natural diamond detectors based D–T neutron spectrometry system," *Rev. Sci. Instrum.* **68**(1), 553–556 (1997).
- <sup>8</sup>M. Pillon, M. Angelone, and A. V. Krasilnikov, "14 MeV neutron spectra measurements with 4% energy resolution using a type IIa diamond detector," *Nucl. Instrum. Methods Phys. Res. B* **101**(4), 473–483 (1995).
- <sup>9</sup>M. Angelone, M. Pillon, L. Bertalot, F. Orsitto, M. Marinelli, E. Milani, G. Pucella *et al.*, "Time dependent 14MeV neutrons measurement using a polycrystalline chemical vapor deposited diamond detector at the JET tokamak," *Rev. Sci. Instrum.* **76**(1), 013506 (2005).
- <sup>10</sup>A. Zimbal, L. Giacomelli, R. Nolte, and H. Schuhmacher, "Characterization of monoenergetic neutron reference fields with a high resolution diamond detector," *Radiat. Meas.* **45**(10), 1313–1317 (2010).
- <sup>11</sup>M. Pillon, M. Angelone, A. Krása, A. J. M. Plompen, P. Schillebeeckx, and M. L. Sergi, "Experimental response functions of a single-crystal diamond detector for 5–20.5 MeV neutrons," *Nucl. Instrum. Methods Phys. Res. A* **640**(1), 185–191 (2011).
- <sup>12</sup>M. Rebai, A. Milocco, L. Giacomelli, E. Perelli Cippo, M. Tardocchi, A. Fazzi, A. Pietropaolo, and G. Gorini, "Response of a single-crystal diamond detector to fast neutrons," *J. Instrum.* **8**(10), P10007 (2013).
- <sup>13</sup>M. Angelone, D. Lattanzi, M. Pillon, M. Marinelli, E. Milani, A. Tucciarone, G. Verona-Rinati *et al.*, "Development of single crystal diamond neutron detectors and test at JET tokamak," *Nucl. Instrum. Methods Phys. Res. A* **595**(3), 616–622 (2008).
- <sup>14</sup>H. Sjöstrand, L. Giacomelli, E. A. Sundén, S. Conroy, G. Ericsson, M. G. Johnson, C. Hellesen *et al.*, "New MPRu instrument for neutron emission spectroscopy at JET," *Rev. Sci. Instrum.* **77**(10), 10E717 (2006).
- <sup>15</sup>E. Andersson Sundén, H. Sjöstrand, S. Conroy, G. Ericsson, M. Gatu Johnson, L. Giacomelli, C. Hellesen *et al.*, "The thin-foil magnetic proton recoil neutron spectrometer MPRu at JET," *Nucl. Instrum. Methods Phys. Res. A* **610**(3), 682–699 (2009).
- <sup>16</sup>G. Ericsson, L. Ballabio, S. Conroy, J. Frenje, H. Henriksson, A. Hjalmarsson, J. Källne, and M. Tardocchi, "Neutron emission spectroscopy at JET—results from the magnetic proton recoil spectrometer," *Rev. Sci. Instrum.* **72**(1), 759–766 (2001).
- <sup>17</sup>L. Giacomelli, E. Andersson Sundén, S. Conroy, G. Ericsson, M. Gatu Johnson, C. Hellesen, A. Hjalmarsson *et al.*, "Development and characterization of the proton recoil detector for the MPRu neutron spectrometer," *Rev. Sci. Instrum.* **77**(10), 10E708 (2006).
- <sup>18</sup>See <http://mcnpx.lanl.gov/> for MCNPX code.
- <sup>19</sup>M. G. Johnson, L. Giacomelli, A. Hjalmarsson, M. Weiszflog, E. A. Sundén, S. Conroy, G. Ericsson *et al.*, "The TOFOR neutron spectrometer and its first use at JET," *Rev. Sci. Instrum.* **77**(10), 10E702 (2006).
- <sup>20</sup>A. Hjalmarsson, S. Conroy, G. Ericsson, L. Giacomelli, G. Gorini, H. Henriksson, J. Källne, M. Tardocchi, and M. Weiszflog, "The TOFOR spectrometer for 2.5 MeV neutron measurements at JET," *Rev. Sci. Instrum.* **74**(3), 1750–1752 (2003).
- <sup>21</sup>M. G. Johnson, L. Giacomelli, A. Hjalmarsson, J. Källne, M. Weiszflog, E. Andersson Sundén, S. Conroy *et al.*, "The 2.5-MeV neutron time-of-flight spectrometer TOFOR for experiments at JET," *Nucl. Instrum. Methods Phys. Res. A* **591**(2), 417–430 (2008).
- <sup>22</sup>See [www.cividec.at](http://www.cividec.at/) for CIVIDEC.
- <sup>23</sup>See <http://www.caen.it/cs/ite/CaenProd.jsp?parent=14&idmod=632> for CAEN — Costruzioni Apparecchiature Elettroniche Nucleari S.p.A., DT5751 2/4 channel 10 bit 2/1 GS/s digitizer.
- <sup>24</sup>V. T. Jordanov, G. F. Knoll, A. C. Huber, and J. A. Pantazis, "Digital techniques for real-time pulse shaping in radiation measurements," *Nucl. Instrum. Methods Phys. Res. A* **353**(1), 261–264 (1994).
- <sup>25</sup>D. B. Syme, S. Popovichev, S. Conroy, I. Lengar, and L. Snoj, "Fusion yield measurements on JET and their calibration," *Nucl. Eng. Des.* **246**, 185–190 (2012).
- <sup>26</sup>See <http://atom.kaeri.re.kr/> for Cross Section Database.
- <sup>27</sup>G. F. Knoll, *Radiation Detection and Measurements* (John Wiley and Sons, New York, NY, 1979).
- <sup>28</sup>J. Frenje, L. Ballabio, S. Conroy, G. Ericsson, M. Tardocchi, E. Traneus, J. Källne, and G. Gorini, "Neutron spectrometry of triton burn-up in plasmas of deuterium," *Plasma Phys. Controlled Fusion* **40**(7), 1211 (1998).
- <sup>29</sup>L. Ballabio, J. Frenje, J. Källne, S. W. Conroy, G. Ericsson, M. Tardocchi, E. Traneus, and G. Gorini, "Measurement and interpretation of the spectrum of the triton burnup neutron emission from deuterium tokamak plasmas," *Nucl. Fusion* **40**(1), 21 (2000).
- <sup>30</sup>H. Sjöstrand, G. Giuseppe, C. Sean, E. Göran, L. Giacomelli, H. Henriksson, A. Hjalmarsson *et al.*, "Triton burn-up neutron emission in JET low current plasmas," *J. Phys. D: Appl. Phys.* **41**(11), 115208 (2008).
- <sup>31</sup>W. Cash, "Parameter estimation in astronomy through application of the likelihood ratio," *Astrophys. J.* **228**, 939–947 (1979).
- <sup>32</sup>M. Tardocchi, M. Nocente, I. Proverbio, V. G. Kiptily, P. Blanchard, S. Conroy, M. Fontanesi *et al.*, "Spectral broadening of characteristic  $\gamma$ -ray emission peaks from C 12 (He 3, p  $\gamma$ ) N 14 reactions in fusion plasmas," *Phys. Rev. Lett.* **107**(20), 205002 (2011).
- <sup>33</sup>M. Nocente, M. Tardocchi, V. G. Kiptily, P. Blanchard, I. Chugunov, Sean Conroy, T. Edlington *et al.*, "High-resolution gamma ray spectroscopy measurements of the fast ion energy distribution in JET 4He plasmas" *Nucl. Fusion* **52**(6), 063009 (2012).
- <sup>34</sup>M. Nocente, M. Garcia-Munoz, G. Gorini, M. Tardocchi, A. Weller, S. Akaslopolo, R. Bilato *et al.* "Gamma-ray spectroscopy measurements of confined fast ions on ASDEX Upgrade" *Nucl. Fusion* **52**(9), 094021 (2012).
- <sup>35</sup>Z. Chen, M. Nocente, M. Tardocchi, T. Fan, and G. Gorini, "Simulation of neutron emission spectra from neutral beam-heated plasmas in the EAST tokamak," *Nucl. Fusion* **53**(6), 063023 (2013).
- <sup>36</sup>H. Henriksson, "Neutron spectroscopy studies of heating effects in fusion plasmas," Ph.D. thesis, Acta Universitatis Upsaliensis No. 861 (Faculty of Sciences and Technology, Uppsala University, 2003).
- <sup>37</sup>H. Klein, "Neutron spectrometry in mixed fields: NE213/BC501A liquid scintillation spectrometers," *Radiat. Prot. dosim.* **107**(1–3), 95–109 (2003).
- <sup>38</sup>F. Gagnon-Moisan, M. Reginatto, and A. Zimbal, "Results for the response function determination of the Compact Neutron Spectrometer," *J. Instrum.* **7**(03), C03023 (2012).

- <sup>39</sup>L. Giacomelli, S. Conroy, F. Belli, G. Gorini, L. Horton, E. Joffrin, E. Lerche, A. Murari, S. Popovichev, M. Riva, and B. Syme, International Conference on Fusion Reactor Diagnostics, Villa Monastero, Varenna, Italy, 9–13 September 2013, see <http://www.iop.org/Jet/fulltext/EFDC130402.pdf>.
- <sup>40</sup>L. Giacomelli, A. Zimbal, K. Tittelmeier, H. Schuhmacher, G. Tardini, R. Neu, and ASDEX Upgrade Team, “The compact neutron spectrometer at ASDEX Upgrade,” *Rev. Sci. Instrum.* **82**(12), 123504 (2011).
- <sup>41</sup>S. Marrone, D. Cano-Ott, N. Colonna, C. Domingo, F. Gramegna, E. M. Gonzalez, F. Gunsing *et al.*, “Pulse shape analysis of liquid scintillators for neutron studies,” *Nucl. Instrum. Methods Phys. Res. A* **490**(1), 299–307 (2002).
- <sup>42</sup>L. Giacomelli, S. Conroy, G. Gorini, L. Horton, A. Murari, S. Popovichev, D. B. Syme, and JET EFDA Contributors, “Tomographic analysis of neutron and gamma pulse shape distributions from liquid scintillation detectors at Joint European Torus,” *Rev. Sci. Instrum.* **85**(2), 023505 (2014).
- <sup>43</sup>C. Helleesen, M. G. Johnson, E. A. Sundén, S. Conroy, G. Ericsson, J. Eriksson, G. Gorini *et al.* “Measurements of fast ions and their interactions with MHD activity using neutron emission spectroscopy” *Nuclear fusion* **50**(8), 084006 (2010).
- <sup>44</sup>M. Gatu Johnson, C. Helleesen, E. Andersson Sundén, M. Cecconello, S. Conroy, G. Ericsson, G. Gorini *et al.* “Neutron emission from beryllium reactions in JET deuterium plasmas with 3He minority,” *Nucl. Fusion* **50**(4), 045005 (2010).
- <sup>45</sup>M. Tardocchi, M. Nocente, and G. Gorini, “Diagnosis of physical parameters of fast particles in high power fusion plasmas with high resolution neutron and gamma-ray spectroscopy,” *Plasma Phys. Controlled Fusion* **55**(7), 074014 (2013).
- <sup>46</sup>M. Nocente *et al.*, “Neutron spectroscopy measurements of tritium beam transport at JET,” *Nucl. Fusion* (submitted).